



Analytical capability of the plasma induced by IR TEA CO₂ laser pulses on copper-based alloys

MILOŠ MOMČILOVIĆ¹, JOVAN CIGANOVIĆ¹, DRAGAN RANKOVIĆ², UROŠ JOVANOVIĆ¹, MILOVAN STOILJKOVIĆ¹, JELENA SAVOVIĆ¹ and MILAN TRTICA^{1*}

¹Vinča Institute of Nuclear Sciences, University of Belgrade, P. O. Box 522, 11001 Belgrade, Serbia and ²Faculty of Physical Chemistry, University of Belgrade, P. O. Box 276, 11001 Belgrade, Serbia

(Received 16 April, revised 11 June, accepted 3 July 2015)

Abstract: The applicability of a nanosecond infrared (IR) transversely excited atmospheric (TEA) CO₂ laser, operating at 10.6 μm and 100 ns pulse length (initial spike), induced plasma under reduced air pressure for spectrochemical analysis of bronze and brass samples was investigated. The plasma consisted of two clearly distinguished and spatially separated regions and expanded to a distance of about 10 mm from the surface. The elemental composition of the samples was determined using a time-integrated space-resolved laser-induced plasma spectroscopic (TISR-LIPS) technique. Sharp and well-resolved spectral lines mostly atomic, and negligibly low background emission, were obtained from a plasma region 7 mm from the target surface. Good signal to background and signal to noise ratios were obtained. The estimated detection limits for the trace elements Mg, Fe, Al and Ca were in the order of 10 ppm in bronze and around 50 ppm in brass. Damage on the investigated samples induced by TEA CO₂ laser radiation was negligible.

Keywords: TEA CO₂ laser; LIBS; copper-based alloys.

INTRODUCTION

Laser-induced breakdown spectroscopy (LIBS) is a powerful analytical technique for rapid analysis of a large variety of materials. A number of works report LIBS application for the analysis of bronze and brass samples,^{1–5} and many of the samples were cultural heritage materials. This is not surprising because copper-based alloys were often used in ancient times and LIBS appears to be the most suitable technique for dating and rapid classification of metal objects.⁶ Nowadays, a variety of techniques, including X-ray photoelectron spectroscopy, X-ray fluorescence and diffraction spectroscopy, Raman spectroscopy, Fourier

*Corresponding author. E-mail: trtica@vinca.rs
doi: 10.2298/JSC150416061M

transform infrared spectroscopy, scanning electron microscopy, inductively-coupled-plasma atomic-emission spectrometry and (laser ablation) inductively-coupled mass spectrometry have been successfully used for the characterization of archaeological objects.^{7,8} Although some of the aforementioned techniques may have better analytical figures of merit (such as accuracy, precision and limits of detection), the specific features of LIBS makes this technique particularly suitable for elemental analysis of cultural heritage objects. LIBS combines the capability of providing fast multi-elemental analysis with no sample pretreatment, potential for *in situ* and remote analysis, micro-destructiveness and the ability to provide isotopic ratio information additionally to elemental composition. Besides, virtually unique to LIBS is the possibility of surface cleaning, analyzing multi-layered samples and performing depth profiling. One of the main difficulties for a precise and accurate quantitative analysis by LIBS is due to matrix effects, to which laser induced plasmas can be very sensitive.

Although various laser systems were used for plasma generation,^{5,9,10} LIBS analysis of copper-based alloys was most often accomplished by means of Nd:YAG lasers. To the best of our knowledge, the possible use of transversely excited atmospheric (TEA) CO₂ laser has not hitherto been examined. There are two main reasons for this. First, the photon energy of CO₂ laser radiation is relatively low (≈ 0.12 eV whereas, for comparison, Nd:YAG laser photon energy is ≈ 1.17 eV). Second, copper strongly reflects the incident light in the infrared spectral range (for CO₂ laser emission wavelength of 10.6 μm , the reflectivity is $\approx 98\%$). Considering the analysis of metal samples, the most critical stage for plasma generation using a TEA CO₂ laser is heating and evaporation of the target. However, once the initial plasma is produced, the long wavelength and long pulse duration of CO₂ laser becomes advantageous. The initial plasma absorbs the remaining laser pulse energy through inverse "Bremsstrahlung" and this absorption is much stronger in the case of a TEA CO₂ laser than for an Nd:YAG laser.¹¹ This is because the plasma absorption coefficient is proportional to the square of the laser wavelength. Thus, when a CO₂ laser is used, appreciable laser heating of the plasma occurs at low density far from the target surface. Consequently, spatial discrimination between line and continuum emission is improved and line broadening reduced. It was shown that under reduced air pressure, plasma could readily be induced by irradiation of a copper target with TEA CO₂ laser peak intensity of 30 MW cm⁻².¹²⁻¹⁴

The aim of the present study was to test the applicability of TEA CO₂ laser induced plasma under reduced air pressure for spectrochemical analysis of copper-based alloys: bronze (Cu–Sn) and brass (Cu–Zn). The obtained results should provide a basis for potential applications of TEA CO₂ laser based LIBS for the analysis of cultural heritage objects made of copper alloys.

EXPERIMENTAL

Schematic diagram of experimental setup used for LIBS analysis of bronze and brass samples is shown in Fig. 1. Plasma was initiated by irradiation of a metal target with a nanosecond infrared (IR) transversely excited atmospheric (TEA) CO₂ laser, operating at 10.6 μm. A typical output pulse energy was 150 mJ, and the repetition rate during the experiments was 1.5 Hz. The laser/optical pulse had a gain switched spike followed by a slowly decaying tail. The full width at half maximum, FWHM, of the spike was about 100 ns while the tail duration was ≈2 μs. The energy sustained in the initial spike was about 35 % of the total irradiated laser energy.

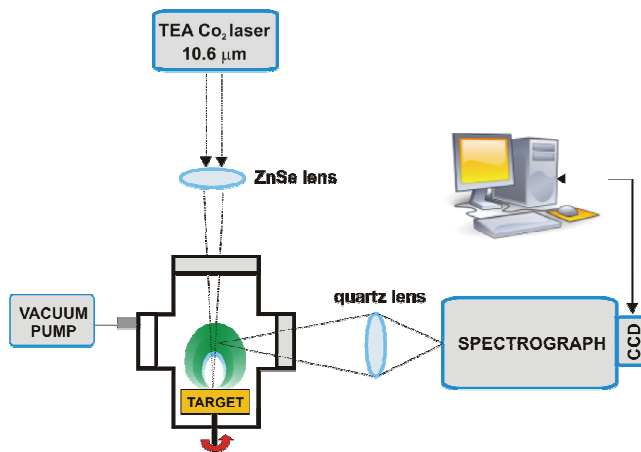


Fig. 1. Schematic diagram of experimental setup used for LIBS analysis of bronze and brass samples.

The samples were placed in a glass vacuum chamber closed with NaCl and CaF₂ windows. The air pressure during the experiments was ≈0.1 mbar. The production of stable and reproducible plasma required a “fresh” area at the target surface between two successive laser pulses, which was achieved by rotation of the sample at 0.5 rpm using a step motor.

The optical emission from the plasma was viewed in the direction parallel to the target surface. By changing the position of the plasma along the direction of the laser beam, while keeping a constant distance between the focusing lens and the target, different parts of the plasma were observed, *i.e.*, a spatial plasma resolution was achieved. The horizontal part of the plume was projected by a lens on the entrance slit of a monochromator (Carl-Zeiss PGS2 dispersion 0.7 nm/mm). For the time-integrated spatially resolved measurements, an Apogee Alta F1007 CCD camera was used. Each emission spectrum was obtained by integration of 30 laser shots impinging on fresh spots of the target.

The high electron density of the plasma immediately after laser ablation gives rise to a strong continuum emission and to broadening of the lines because of the Stark effect. Usually temporal gating of the emission is used in order to discriminate the atomic emission from the continuum background. In this work, time-integrated space-resolved laser induced plasma spectroscopy (TISR-LIPS) was used.^{14,15} This method relies on the fact that the intense plasma background spectral continuum emission is mostly emitted from a region close to the sample surface, while in the further-out regions of the plasma, the continuum emission is

largely reduced. The fact that the plasma reaches a given distance above the analyzed surface with a certain time delay enables replacing temporal with spatial resolution. Thus, instead of time-gated detection, the position-selective spectra were recorded.

RESULTS AND DISCUSSION

The plasma was initiated by irradiation of a copper alloy target with a fluence of $\approx 8.6 \text{ J cm}^{-2}$ in an air atmosphere at a pressure of 0.1 mbar. The plasma consisted of two clearly distinguished and spatially separated regions, Fig. 2. The first region, close to the target surface (length about 5 mm), was characterized by a whitish color and is known as primary plasma. The second region, also known as the secondary plasma, was larger in volume, had a hemispherical shape and intense green color, due to emission of the spectral lines of the target. The plasma expanded to a distance of about 10 mm from the surface.

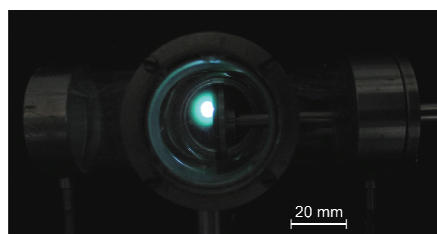


Fig. 2. Image of the plasma induced over a brass sample.

The composition of bronze and brass samples used in this study were determined by inductively coupled plasma atomic emission spectroscopy (ICP-AES), Table I.

TABLE I. Elemental composition of bronze and brass samples; nd: not detected

Sample	Metal											
	Cu	Sn	Zn	Pb	Ni	Ca	Fe	Al	Co	Mg	Mn	Cr
wt. %												
Bronze	56	41	1.7	1.1	0.07	0.04	60	40	32	26	8	6
Brass	69	nd	30	nd	nd	0.23	260	125	nd	300	<5	nd

The time-integrated emission spectra of the major and trace elements present in the bronze and brass samples are shown in Figs. 3 and 4; the optical emission was analyzed in the wavelength region ranging from about 250 to 650 nm, but the LIBS experimental spectra in the most significant wavelength windows are shown. The spectrum consisted of well-resolved sharp emission lines, and low background emission intensity. Good signal to noise and signal to background ratios were obtained. The signal to background, and signal to noise ratios together with the estimated limits of detection (*LOD*) are presented in Table II. The limits of detection were calculated using the formula:

$$LOD = 3BEC \times RSD_B$$

where BEC is the background equivalent concentration and RSD_B is the relative standard deviation of the background.

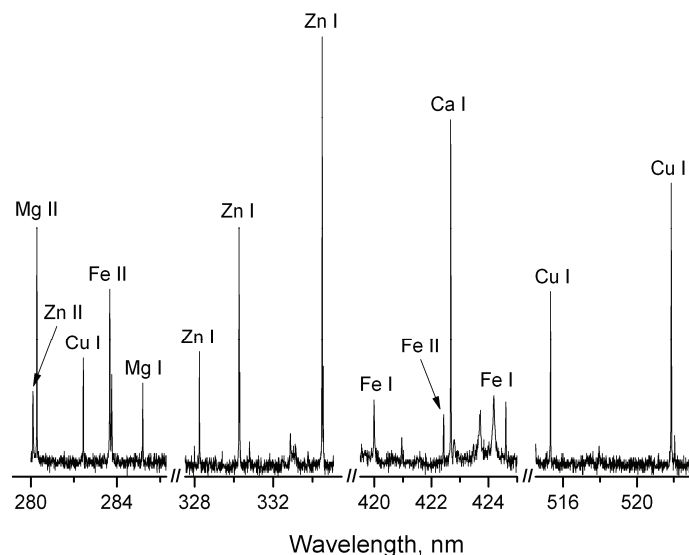


Fig. 3. LIBS spectra of the brass sample. The composition of the sample is given in Table I. The main emission lines are labeled in the spectrum. Air pressure 0.1 mbar, laser fluence 8.6 J cm^{-2} (intensity 30 MW cm^{-2}).

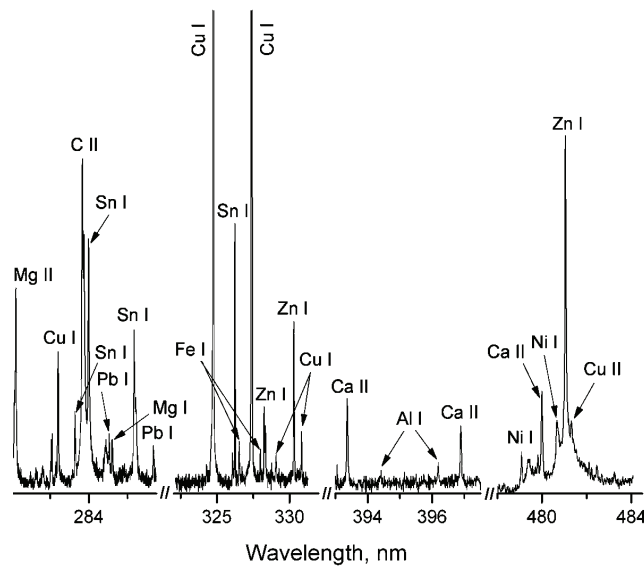


Fig. 4. LIBS spectra of bronze sample. The composition of the sample is given in Table I. The main emission lines are labeled in the spectrum. Air pressure: 0.1 mbar, laser fluence 8.6 J cm^{-2} (intensity 30 MW cm^{-2}).

TABLE II. Signal to noise (*S/N*) and signal to background (*S/B*) ratio, and the estimated limits of detection (*LOD*) for bronze and brass

Element	Wavelength, nm	<i>S/N</i>	<i>S/B</i>	<i>LOD</i> / mg kg ⁻¹
Bronze				
Mg	280.27	40	4	2
Fe	328.02	14	2	13
Al	396.15	9	1	13
Ca	422.67	56	2	21
Brass				
Mg	285.21	26	5	35
Fe	288.13	20	3	40
Al	396.15	30	36	13
Ca	422.67	126	16	55

Higher *LOD* obtained for brass compared to bronze may be a consequence of a matrix effect that leads to variations in the plasma parameters. In the case of metallic samples, stronger matrix effects were found for alloys with high Zn contents, such as brass.^{2,5} Thermal vaporization may significantly influence the ablation processes, especially when the ablation is accomplished by a low power density, long-pulse duration laser, as in the present study.

There are a large number of research papers devoted to the application of LIBS for the analyses of copper-based alloys. However, they are mainly limited to the determination of major elements, while there are still very few works that report *LOD* values for minor or trace elements. Furthermore, different elements were analyzed, thus comparison of the present results with literature data is rather limited. One exception is iron, for which *LOD* values of 22.3¹⁶ and 150 ppm¹⁷ were evaluated for Fe I 372.26 nm and Fe II 234.83 nm lines, respectively. For other minor elements, such as Ag, As, Ni and Pb, the limits of detection were in the range from 1.4 to 250 ppm;^{16,17} in both papers, an Nd:YAG laser and time gated detection (iCCD camera) was used. Limits of detection are element dependent, nevertheless the *LOD* values obtained using TEA CO₂ laser and non-gated detection are of the same order of magnitude (ppm) as the ones obtained with standard LIBS.

Each analytical technique available for the characterization of archaeological objects is characterized by its own strengths and weaknesses. The selection of the most appropriate depends on the analytical problem, on possible limitations imposed by the object or sample examined, and on the capabilities of the technique. Although the *LOD* of a spectral line is an important characteristic, it is just one of many parameters that are considered in the method selection process. For example, the *LOD* values of inductively coupled mass spectrometry are among the lowest (μg–ng per kg), however this method is destructive (the sample to be analyzed must be digested prior to analysis) and could not be used if there is a need for *in situ* analysis. Special features of LIBS, such as rapidity, low invasive-

ness, high spatial discrimination and possibility to perform *in situ* measurements, make this technique quite competitive compared with other techniques commonly used in archaeological science for obtaining information about elemental composition.

An important characteristic of the proposed LIBS system is position-selective emission spectroscopy, which eliminates the need for time-gated detection. This is not a new concept, it was already successfully applied for studying various laser induced plasmas.^{18,19} For instance, Bulatov *et al.*¹⁸ applied non-gated detection for the analysis of brass samples using a Nd:YAG laser (400 mJ, 7 ns, 2.25×10^9 W cm⁻²). Compared to the Nd:YAG laser, the TEA CO₂ laser has a longer wavelength and longer pulse duration. Both these characteristics are favorable for non-gated detection of spectral lines. In general, the dimensions and lifetime of a plasma increase with pulse duration. The plasma takes longer to decay and hence, the emission lasts longer. The leading part of the TEA CO₂ laser pulse (FWHM \approx 100 ns) produces the plasma, while the tail part (\approx 2 μ s) interacts with it by means of laser absorption. Absorption of the laser radiation in the plasma occurs mainly by inverse “Bremsstrahlung”, which increases as the laser wavelength increases.¹¹ Absorption by the plume causes an additional plasma excitation and expansion, which increase the LIBS signal through enhancement of emission lines. Simultaneously, because of the longer wavelength of CO₂ laser radiation, heating of the plasma by optical absorption occurs at lower plasma densities.¹¹ Strong line emission is therefore observed at greater distances from the target surface, where the background is negligibly low. In general, a shorter pulse gives a higher ablation rate, if the pulse energy or the fluence is constant.^{19,20} This means that the higher emission intensities obtained by the elongated pulses do not indicate a higher ablation rate, but rather a higher efficiency of the emission.¹⁸

The goal of this investigation was to test the applicability of a TEA CO₂ laser based LIBS for the analysis of copper alloys, with the intention to (eventually) use this system for the analysis of cultural heritage objects made of bronze and brass. In this regard, it is important to mention that the TEA CO₂ laser radiation induced negligible damage on the investigated samples. Previous results showed that irradiation of a pure copper target with a TEA CO₂ laser intensity of approx. 100 MW cm⁻² under 0.1 mbar air pressure induced only superficial damage, practically invisible in the OM image (magnification 50 \times).¹⁴

Taking all into consideration (compact, low-cost detection system; well-resolved spectral lines; LOD values in the ppm range, typical for LIBS; minimal destructivity), it could be concluded that for the elemental analysis of copper alloys, the proposed LIBS system based on a TEA CO₂ laser may be a suitable alternative to conventional LIBS using an Nd:YAG laser.

CONCLUSIONS

The plasma was induced by irradiation of a copper alloy target with 30 MW cm⁻² of TEA CO₂ laser peak intensity, in air at 0.1 mbar. Time-integrated emission spectra of elements present in the bronze and brass samples were used for an evaluation of the signal to background and signal to noise ratios, and an estimation of the limits of detection. Detection limits for trace elements were in the order of 10 ppm in brass and around 50 ppm in bronze. The single-shot TEA CO₂ LIBS has significant potential for cultural heritage applications.

Acknowledgement. This work was supported by the Ministry of Education, Science and Technological Development of the Republic Serbia, Project No. 172019.

ИЗВОД

ПЛАЗМА ИНДУКОВАНА ИНФРАЦРВЕНИМ ТЕА CO₂ ЛАСЕРОМ НА ЛЕГУРАМА БАКРА
– МОГУЋНОСТИ АНАЛИТИЧКЕ ПРИМЕНЕ

МИЛОШ МОМЧИЛОВИЋ¹, ЈОВАН ЦИГАНОВИЋ¹, ДРАГАН РАНКОВИЋ², УРОШ ЈОВАНОВИЋ¹, МИЛОВАН СТОИЉКОВИЋ¹, ЈЕЛЕНА САВОВИЋ¹ и МИЛАН ТРТИЦА¹

¹Институција за нукеларне науке Винча, Универзитет у Београду, 11001 Београд и ²Факултет за физичку хемију, Универзитет у Београду, Студентски ћард 12–16, 11001 Београд

Испитана је могућност спектрохемијске примене плазме индуковане дејством зрачења импулсног TEA CO₂ ласера (10,6 μm, 100 nm) на мете од бронзе и месинга. Димензија плазме индуковане на сниженом притиску ваздуха износила је 10 mm са јасно израженим и просторно раздвојеним областима. Елементни састав узорака одређен је временски интегралјеном просторно разложеном емисионом спектроскопијом ласерски индуковане плазме (TISR-LIPS). Оштре и добро разложене спектралне линије (углавном атомске), уз занемарљиво ниску емисију позадине, добијене су посматрањем плазме на растојању 7 mm од површине мете. Такође, добијен је добар однос линије према позадини и линије према шуми. Добијене границе детекције за елементе у трајовима, Mg, Fe, Al и Ca, биле су реда величине око 10 ppm у бронзи и око 50 ppm у месингу. Оштећења настала дејством ласерског TEA CO₂ зрачења на испитиваним узорцима била су незнатна.

(Примљено 16. априла, ревидирано 11. јуна, прихваћено 3. јула 2015)

REFERENCES

1. F. Colao, R. Fantoni, V. Lazic, V. Spizzichino, *Spectrochim. Acta, B* **57** (2002) 1219
2. L. Fornarini, R. Fantoni, F. Colao, A. Santagata, R. Teghil, A. Elhassan, M. A. Harith, *J. Phys. Chem., A* **113** (2009) 14364
3. F. J. Fortes, M. Cortes, M. D. Simon, L. M. Cabalín, J. J. Laserna, *Anal. Chim. Acta* **554** (2005) 136
4. A. A. Shaltout, M. S. Abdel-Aal, N. Y. Mostafa, *J. Appl. Spectrosc.* **78** (2011) 594
5. V. Margetic, A. Pakulev, A. Stockhaus, M. Bolshov, K. Niemax, R. Hergenroder, *Spectrochim. Acta, B* **55** (2000) 1771
6. R. Gaudioso, M. Dell'Aglio, O. De Pascale, G. S. Senesi, A. De Giacomo, *Sensors* **10** (2010) 7434
7. E. Ciliberto, G. Spoto, Eds., *Modern Analytical Methods in Art and Archaeology*, Wiley/Interscience, New York, 2000

8. A. Giakoumaki, K. Melessanaki, D. Anglos, *Anal. Bioanal. Chem.* **387** (2007) 749
9. A. Elhassan, A. Giakoumaki, D. Anglos, G. M. Ingo, L. Robbiola, M. A. Harith, *Spectrochim. Acta, B* **63** (2008) 504
10. A. De Giacomo, M. Dell'Aglio, O. De Pascale, R. Gaudiose, R. Teghil, A. Santagata, G. P. Parisi, *Appl. Surf. Sci.* **253** (2007) 7677
11. A. Khumaeni, Z. S. Lie, H. Niki, K. H. Kurniawan, E. Tjoeng, Y. I. Lee, K. Kurihara, Y. Deguchi, K. Kagawa, *Anal. Bioanal. Chem.* **400** (2011) 3279
12. M. Momcilovic, M. Trtica, J. Ciganovic, J. Savovic, J. Stasic, M. Kuzmanovic, *Appl. Surf. Sci.* **270** (2013) 486
13. M. Kuzmanovic, M. Momcilovic, J. Ciganovic, D. Rankovic, J. Savovic, D. Milovanovic, M. Stoiljkovic, M. S. Pavlovic, M. Trtica, *Phys. Scr. T.* **162** (2014) 014011
14. M. Momcilovic, M. Kuzmanovic, D. Rankovic, J. Ciganovic, M. Stoiljkovic, J. Savovic, M. Trtica, *Appl. Spectrosc.* **69** (2015) 419
15. M. A. Khater, P. van Kampen, J. T Costello, J. P. Mosnier, E. T. Kennedy, *J. Phys., D: Appl. Phys.* **33** (2000) 2252
16. M. Sababi, P. Cielo, *J. Anal. At. Spectrom.* **10** (1995) 643
17. F. J. Fortes, M. Cortes, M. D. Simon, L. M. Cabalín, J. J. Laserna, *Anal. Chim. Acta* **554** (2005) 136
18. V. Bulatov, R. Krasniker, I. Schechter, *Anal. Chem.* **72** (2000) 2987
19. A. Matsumoto, A. Tamura, K. Fukami, Y. H. Ogata, T. Sakka, *Anal. Chem.* **85** (2013) 3807
20. T. Sakka, H. Oguchi, S. Masai, K. Hirata, Y. H. Ogata, M. Saeki, H. Ohba, *Appl. Phys. Lett.* **88** (2006) 061120.